

Prognostic value of genome-wide DNA methylation patterns in noncoding miRNAs and lncRNAs in uveal melanomas

Zheng Zheng^{1,*}, Dan Xu^{1,*}, Keqing Shi², Minfeng Chen¹, Fan Lu¹

¹School of Ophthalmology and Optometry, Eye Hospital, Wenzhou Medical University, State Key Laboratory and Key Laboratory of Vision Science, Ministry of Health and Zhejiang Provincial Key Laboratory of Ophthalmology and Optometry, Wenzhou, Zhejiang 325000, China

²The First Affiliated Hospital of Wenzhou Medical University, Wenzhou, Zhejiang 325000, China

*Equal contribution

Correspondence to: Fan Lu; email: lufan62@mail.eye.ac.cn

Keywords: UVMs, miRNAs, lncRNAs, methylated panel, prognostic value

Received: January 15, 2019

Accepted: August 9, 2019

Published: August 20, 2019

Copyright: Zheng et al. This is an open-access article distributed under the terms of the Creative Commons Attribution License (CC BY 3.0), which permits unrestricted use, distribution, and reproduction in any medium, provided the original author and source are credited.

ABSTRACT

Background: Uveal melanomas are the most common primary intraocular malignant tumors in adults, associated with a high metastasis rate and a low 5-year survival rate. It is a clinic urgency and importance to identify prognostic factors for UVMs.

Results: 55 aberrantly methylated sites of miRNAs and 47 aberrantly methylated sites of lncRNAs were observed between Alive < 2 years group and Alive > 2 years group of UVMs. Two prognostic classifiers were generated. For 13- miRNAs-CpG-classifier, the AUC were 0.958, 0.848 and 0.824 at 1 year, 2 years and 3 years, respectively. For 9- lncRNAs-CpG-classifier, the AUC were 0.943, 0.869 and 0.866 at 1 year, 2 years and 3 years, respectively.

Conclusion: The correlation between genome-wide DNA methylation patterns of miRNAs and lncRNAs and the overall survival in UVMs were identified in this study. This novel finding shed new light on developing biomarkers of prognosis for UVMs.

Methods: DNA methylation profiles of noncoding miRNAs and lncRNAs for UVMs were accessed from The Cancer Genome Atlas. Then the prognostic value was analyzed by least absolute shrinkage and selection operator method Cox regression and tested by Time-dependent Receiver Operating Characteristic curve.

INTRODUCTION

Uveal melanomas (UVMs) which come from melanocytes in the choroid layer of the eye is the most common primary intraocular malignant tumors in adults [1]. Two main types of UVMs are identified due to behavioral and anatomical differences. Less than 5% of UVMs are iris melanomas, and iris melanomas are less likely to metastasize which are more in common with cutaneous melanomas [2, 3]. Around 95% of UVMs are collectively referred to as posterior UVMs, which are

specific to people with light skin and blue eyes and have a higher rate of metastasis. Approximately 50% of patients of UVMs turn to metastases and the 5-year survival rate is about 15–50% [4–6]. Unfortunately, there is no effective cure for metastatic UVMs nowadays. The molecular mechanisms of metastasis are not fully understood [7]. It is clinic importance to search prognostic factors for UVMs at the molecular level.

MiRNAs are small non-coding RNAs (approximately 22 nucleotides) and the functions of miRNAs are RNA

silencing and post-transcriptional regulation of gene expression [8, 9]. lncRNAs are transcripts longer than 200 nucleotides that are not translated into protein [10]. Similar to mRNAs, lncRNAs are spliced, capped, and polyadenylated. miRNAs are important regulators of gene expression and are frequently dysregulated in cancer [11], and the co-expression pan-cancer analysis revealed that the lncRNAs are frequently co-expressed with cancer genes in multiple cancers [12–15]. It has been reported that miRNAs, such as microRNA-182, miR-9, MicroRNA-34a, microRNA-137, and MiR-140, can inhibit UVMs via the process of proliferation, migration, invasiveness and cell cycle [16–20]. Likewise, lots of lncRNAs are identified dysregulated in the uveal melanoma cells, such as MALAT1 and PAUPAR, which are related to UVMs cell proliferation, colony information, invasion and migration and tumor metastasis [20, 21].

Aberrant hypermethylation of promoter CpG islands and subsequent inactivation of key tumor suppressor genes are a frequent step in tumorigenesis of most human cancers [22–24]. DNA methylation not only suppresses the expression of protein-encoding genes but also affects miRNAs and lncRNAs expression. Aberrant DNA methylation is an epigenetic mechanism that is involved in the process of miRNAs and lncRNAs dysregulation [25]. The associations between aberrant DNA methylation events and the silencing of individual miRNAs and lncRNAs have been demonstrated in many cancer types [26–28].

Some previous studies found that DNA methylation of some protein-encoding genes has been proved to be associated with the development, progression, and metastasis of UVMs [29]. However, little is known about the regulatory mechanisms of miRNAs and lncRNAs regulation by DNA methylation in UVMs, which has been proved to be crucial mechanisms in many other cancers. In this study, we developed methylated panels of miRNAs and lncRNAs, data from 79 UVMs patients. Bioinformatic functional analysis and prognostic value of differentially methylated miRNAs and lncRNAs were also performed (Figure 1).

RESULTS

Data were obtained from 79 UVMs patients in TCGA (Table 1). The clinical characteristics of patients with UVMs were summarized in Table 1. The patients were divided into two groups according to the survival time, live less than 2 years (Alive < 2 years) and live more than 2 years (Alive > 2 years). The Alive < 2 years group had an older median age (74.1 years old) than that (57.5 years old) of Alive > 2 years group ($P < 0.001$). The recurrence rate of Alive < 2 years group was 100%, compared with

24.3% in Alive > 2 years group. No other significant difference was found between Alive < 2 years group and Alive > 2 years group in aspects of gender, epithelioid, largest basal diameter, tumor thickness, TNM staging system, and AJCC pathological stage.

According to the annotation of 450k Chip by TCGA, 4160 CpG sites of miRNA and 11479 CpG sites of lncRNA were screened out. There were 55 CpG sites of miRNA and 47 CpG sites of lncRNA with differential methylation between UVM patients after diagnosis Alive < 2 years group and Alive > 2 years group, within which 45 CpG sites of miRNA and 33 CpG sites of lncRNA had the difference beta-values were greater than 0.1. Hierarchical clustering (HC) analysis of 57 tissues from UVMs with different survival time with different CpG sites of miRNAs and lncRNAs was performed (Figure 2). To identify the biological processes or pathways potentially regulated by differentially methylated miRNA target genes, we applied the miRNA target prediction algorithm and functional annotation analysis. A total of 6109 predicted target genes were identified, and the results showed that GO terms were enriched significantly, which are mainly related to positive regulation of cell development and signaling pathway (biological process, BP), and transcription regulator activity, protein kinase activity and DNA binding (molecular function, MF), and dendrite, cell body, synapse and axon (cellular component, CC). Significantly enriched pathway included the PI3K-Akt signaling pathway, and mitogen-activated protein kinase (MAPK) signaling pathway (Figure 3). In order to explore the potential functions of the differentially methylated genes co-expressed with the lncRNAs, a total of 4012 predicted co-expressed genes were identified using MEM analysis. The results showed that GO terms were enriched significantly, which are related to sequence-specific DNA binding, regulation of ion transmembrane transport, cell junction, multicellular organism development, chemical synaptic transmission and integral component of the plasma membrane. The significantly enriched pathway includes Neuroactive ligand-receptor interaction, cAMP signaling pathway and calcium signaling pathway (Figure 4). We also predicted the interaction of lncRNA signature with miRNA signature and found some gene symbols of lncRNAs interacted with one or more than one gene symbols of miRNAs (Supplementary Table 1). For instance, lncRNA gene symbol MEG8 was predicted to have interaction with miRNA gene symbol miR-379, and lncRNA gene symbol TUNAR was predicted to have interaction with miRNA gene symbol miR-5193 and miR-6754.

In addition, we used a LASSO Cox regression model to build a prognostic classifier, which selected 13 miRNA CpG sites from the 45 miRNA CpG sites: cg00182416,

Table 1. Clinical characteristics of patients in The Cancer Genome Atlas.

Clinicopathological variables	Total (n = 79)	Alive < 2 years (n = 12)	Alive > 2 years (n = 45)	P value
Age				
Median	61.8 (22–86)	74.1 (64–86)	57.5 (22–78)	< 0.001
Gender				
Male	34 (43.0%)	10 (83.3%)	24 (53.3%)	0.097
Female	45 (57.0%)	2 (16.7%)	21 (46.7%)	
Histology				
Epithelioid	12 (15.2%)	3 (25.0%)	6 (13.3%)	0.236
Spindle	30 (38.0%)	2 (16.7%)	19 (42.2%)	
Mixed	37 (46.8%)	7 (58.3%)	20 (44.4%)	
Largest basal diameter (mm)				
Median	16.9 (7.8–25)	18.3 (13.9–25)	16.84 (10.8–25)	0.165
Tumor thickness (mm)				
Median	10.4 (4–16)	11.1 (4–16)	10.5 (5–15)	0.489
TNM staging system (T)				
T1+T2	14 (17.7%)	1 (8.3%)	6 (13.3%)	1.000
T3+T4	65 (82.3%)	11 (91.7%)	39 (86.7%)	
AJCC pathological stage				
I + II	39 (50.0%)	5 (41.7%)	20 (45.5%)	0.815
III + IV	39(50.0%)	7 (58.3%)	24 (54.5%)	
Recurrence	13/60 (21.7%)	1/1 (100%)	9/37 (24.3%)	0.263
Death	22/79 (27.8%)	12/12 (100%)	10/45 (22.2%)	< 0.001

TCGA, The Cancer Genome Atlas.

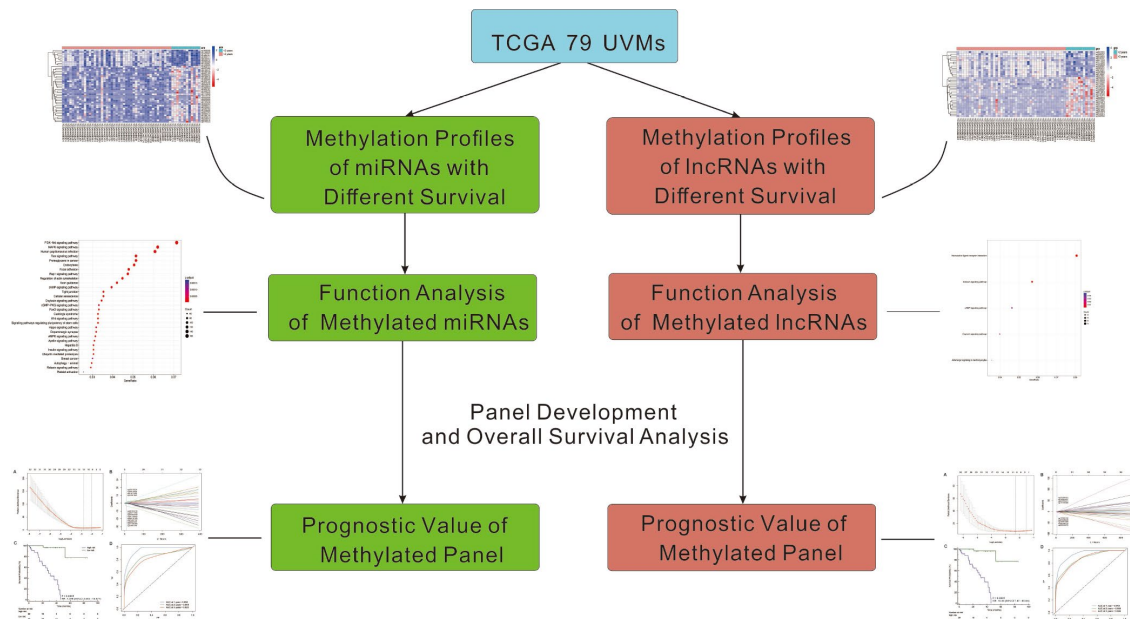


Figure 1. The workflow of this work.

cg05684371, cg07815521, cg09318158, cg11444828, cg13972491, cg14601621, cg15186488, cg18007341, cg21492137, cg23492249, cg24128045 and cg26371705 (Figure 5A, 5B, Supplementary Figures 1, 2 and Supplementary Table 2), and 4 of the 13 selected CpG sites were hypermethylated while 9 of the 13 selected CpG sites were hypomethylated. We also selected 9 lncRNA CpG sites from the 33 lncRNA CpG sites: g01498249, cg04783231, cg09098720, cg11316386, cg14011368, cg14981637, cg17948136, cg20059151 and

cg22232978 (Figure 6A, 6B, Supplementary Figures 5, 6 and Supplementary Table 3), and 2 of the 9 selected CpG sites were hypermethylated while 7 of the 9 selected CpG sites were hypomethylated. A risk score was calculated for each patient based on their methylation levels of the 13 miRNAs' CpG sites: $-(0.0615621 \times \text{status of cg00182416}) - (0.5117782 \times \text{status of cg05684371}) + (0.6512553 \times \text{status of cg07815521}) - (0.226421 \times \text{status of cg09318158}) + (0.64929233 \times \text{status of cg11444828}) + (0.13455497 \times \text{status of cg13972491}) +$

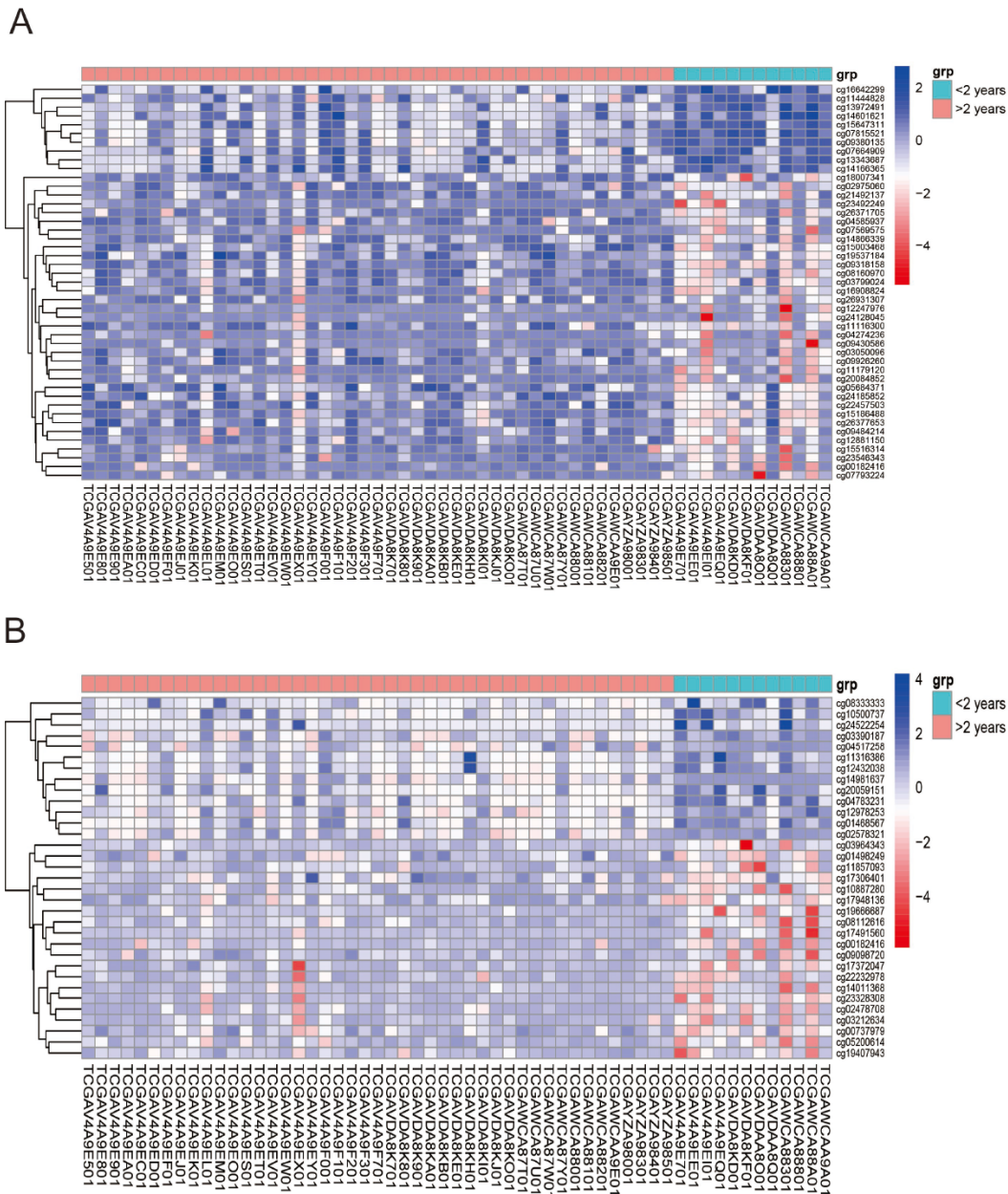


Figure 2. Unsupervised hierarchical cluster in the analysis of differentially methylated miRNAs target genes (A) and genes co-expressing with lncRNAs (B) in UVMs Alive < 2 years group relative to Alive > 2 years group control. Values from samples are presented horizontally, left (red) for Alive > 2 years patients while the right (green) for Alive < 2 years patients. CpG sites of miRNAs and lncRNAs are listed vertically. Blue and red represent levels of hypomethylation and hypermethylation, respectively, while white indicates methylation was not detected.

$(0.04442819 \times \text{status of cg14601621}) - (0.6988188 \times \text{status of cg15186488}) - (2.3256628 \times \text{status of cg18007341}) - (0.3297994 \times \text{status of cg21492137}) - (0.089017 \times \text{status of cg23492249}) - (0.1368466 \times \text{status of cg24128045}) - (0.0712472 \times \text{status of cg26371705})$ (Supplementary Figures 3, 4 and Supplementary Table 4), and the risk score formula based on the methylation level of the 9 lncRNAs' CpG sites = $-(0.76801785 \times \text{status of g01498249}) + (0.11549443 \times \text{status of cg04783231}) - (1.69231163 \times \text{status of cg09098720}) + (0.12727885 \times \text{status of cg11316386}) - (0.14438115 \times \text{status of cg14011368}) - (0.26094577 \times \text{status of cg14981637}) - (0.10594807 \times \text{status of cg17948136}) - (0.18976153 \times \text{status of cg20059151}) - (2.10961601 \times \text{status of cg22232978})$ (Supplementary Figures 7, 8 and Supplementary Table 5) (status meant hypermethylated or hypomethylated degree). In these formulas, the median of the risk scores was used to divide UVMs into high-risk and low-risk groups. When we assessed the distribution of risk scores and survival status, patients with lower risk

scores generally had better survival than those with higher risk scores. This was confirmed by both 13-miRNAs-CpG-classifier (hazard ratio [HR] 7.08, 95% CI 3.00-16.68; $p < 0.0001$; Figure 4C) and 9-aberrantly-methylated-based-lncRNAs-classifier (hazard ratio [HR] 18.95, 95% CI 7.87-45.64; $p < 0.0001$; Figure 5C). We assessed the prognostic accuracy of the 13- miRNAs-CpG-classifier and 9- lncRNAs-CpG-classifier with tdROC analysis at varying follow-up times (Figures 5D, 6D). Although HC analysis was performed in 57 patients due to the beta-values greater than 0.1, the prognosticators were used in all patient samples and predicted survival accurately. For 13- miRNAs-CpG-classifier, the AUC were 0.958, 0.848 and 0.824 at 1 year, 2 years and 3 years, respectively. For 9- lncRNAs-CpG-classifier, the AUC were 0.943, 0.869 and 0.866 at 1 year, 2 years and 3 years, respectively. These results indicate that our aberrantly-methylated-based-classifiers could successfully identify patients' survival probability with UVMs, respectively.

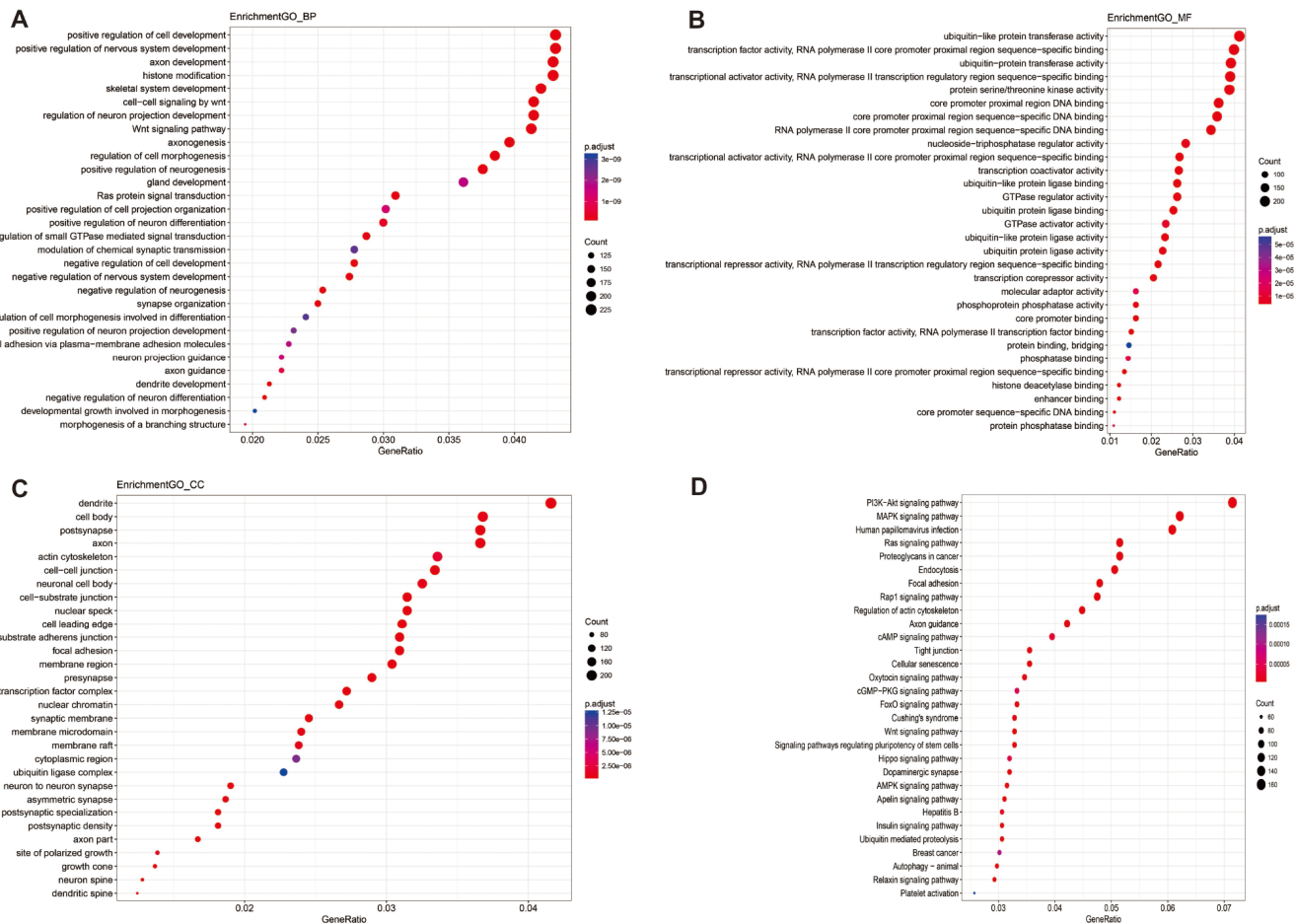


Figure 3. Enriched GO_BP (A), GO_MF (B), GO_CC (C) and KEGG pathway annotation of differentially methylated miRNAs targeted genes. Genes targeted by differentially methylated miRNAs were enriched and annotated for the categories biological process, molecular function, cellular component, and KEGG pathway. Enriched gene ratio was presented horizontally, while the names of protein-coding genes were listed vertically. The color of the dots presented the p.adjust and the size of the dots presented the count of DEG.

DISCUSSION

In the current study, prognosis related genome-wide methylation patterns of miRNAs and lncRNAs were identified in patients with UVMs. Based on the methylation analysis of miRNAs and lncRNAs in UVMs from TCGA and LASSO Cox regression, two aberrantly-methylated-based miRNAs and lncRNAs classifiers were established. Both of them can predict the overall survival of UVMs. MiRNAs target about 60% of the human genes and many miRNAs are evolutionarily conserved, implying its important biological functions [30]. MiRNAs combine with complementary sequences of mRNAs via base-pairing to silence these mRNAs, cleaving mRNAs into pieces, shortening the poly(A) tail of mRNAs and decreasing translation of mRNAs [31, 32]. Although non-protein-coding, it is suggested that the majority of lncRNAs are supposed to be functional [33] and a small proportion has been demonstrated to be biologically relevant, including regulation of gene expression, dosage compensation, genomic imprinting, nuclear organization

and compartmentalization, and nuclear to cytoplasmic trafficking [34]. Methylation is an important component of the repression of relevant genes in cells, including the miRNAs and lncRNAs. In many cancer types, aberrant DNA methylation was associated with the silencing of individual miRNAs and lncRNAs. In this study, the methylation of CpG sites related to miRNAs and lncRNAs were demonstrated in different survival time groups of UVMs, which could induce loss of expression of genes more frequently than by mutations, and DNA methylation is recognized to be a chief contributor to the stability of gene expression states [35].

Aberrant methylation of miRNAs and lncRNAs can perturb specific biological processes or pathways. The results of function annotation showed that the aberrant methylation of sites targeted miRNAs can influence malignancy related pathways, including the regulation of cell development, transcription, protein kinase activity, DNA binding, cellular component (dendrite, cell body, synapse, and axon) and PI3K-Akt signaling pathway,

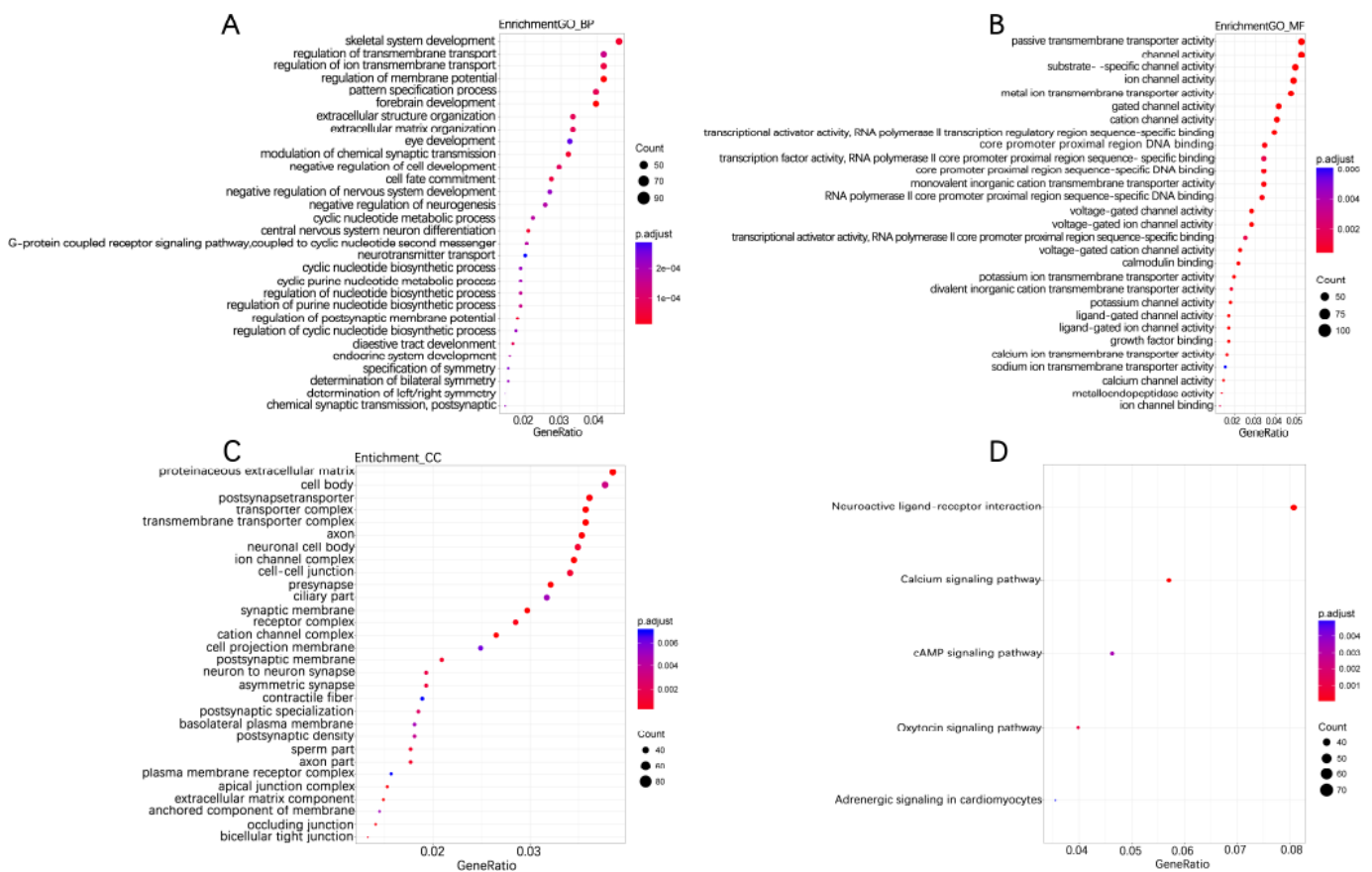


Figure 4. Enriched GO_BP (A), GO_MF (B), GO_CC (C) and KEGG pathway annotation of differentially methylated genes co-expressing with lncRNAs. Differentially methylated Genes co-expressing with lncRNAs were enriched and annotated for the Gene Ontology and KEGG pathway. Enriched gene ratio was presented horizontally, while the names of protein-coding genes were listed vertically. The color of the dots presented the $-\log_{10}(\text{FDR})$ and the size of the dots presented the Gene number.

MAPK signaling pathway, Ras signaling pathway. PI3Ks locate at the inner of the plasma membrane and can generate the second messenger phosphatidylinositol-3,4,5-trisphosphate (PI-3, 4, 5-P (3)). Then through the activation of the phospholipids produced by PI3Ks, Akt modulates can activate the function of numerous substrates involved in the regulation of cell survival, cycle progression, and cellular growth. Recent studies have shown that the PI3K/Akt signaling pathway components are frequently altered in human cancers [36]. Furthermore, compared to any other pathway in cancer patients, the components of PI3K/Akt pathway are targeted by amplification, mutation, and translocation more frequently, exploiting this pathway a promising candidate for cancer drug discovery [37]. MAPK pathway in physiologic conditions regulates cell growth, survival, and migration, transducing cell-surface signals

to the nucleus via phosphorylation. The dysregulation of the MAPK signaling pathway is common in many human cancers via constitutive activation, including melanoma [38]. For the Ras signaling pathway, the activation of RAS is through the effector proteins such as RAF, PI3K, protein kinase C- [zeta] and phospholipase- [varepsilon], and it will subsequently initiate MAPK signaling pathway too [39]. The results of functional annotation of lncRNAs showed that the aberrant methylation of sites that co-expressed with lncRNAs can influence the functions related to sequence-specific DNA binding, regulation of ion transmembrane transport, cAMP signaling pathway, and calcium signaling pathway. Misregulation of local cyclic AMP (cAMP) signaling proved to have pathophysiological consequences, including cancer [40] and can act as a promising cellular target for antitumor treatments [41, 42]. Ca²⁺ is a second

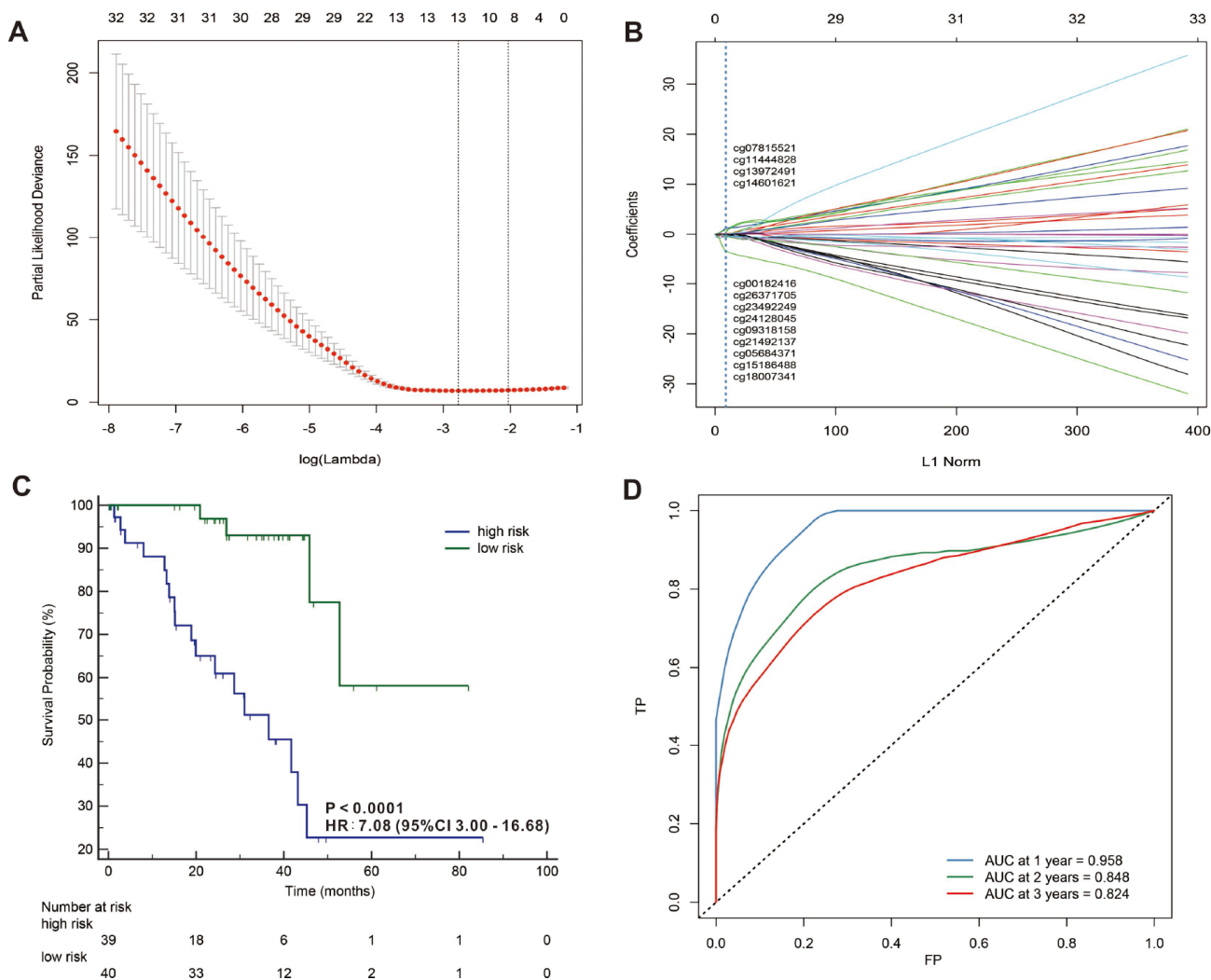


Figure 5. LASSO coefficient profiles of the 32 UVMs-associated miRNAs (A, B). Kaplan-Meier survival analysis for all 79 patients with UVMs according to the 13-miRNAs-classifier stratified by clinicopathological risk factors (C). Time-dependent ROC curves by 13-miRNAs-classifier for survival probability (D).

messenger of the activation or inhibition of several signaling pathways [43]. The deregulation of Ca²⁺ homeostasis results in tumorigenesis, including proliferation, angiogenesis, apoptosis, and gene transcription and several cancers are closely connected with Ca²⁺ channels and pumps [44].

The prognosis results of patients with metastatic UVMs were very poor, the median survival time after clinical detection of metastases was only 9 months [45]. Once after metastasis, there is no effective treatment for UVMs. Thus, diagnosing UVMs at an early stage is crucial to reduce the mortality, which requires reliable prognostic indicators. Kujala E et al. investigated the clinical characteristics in long-term prognosis of patients with UVM, indicating that the original histopathologic diagnosis was correct in 91%, but 10% biopsy diagnosis and 7% autopsy diagnosis were changed by immunohistochemical reassessment [46]. Robertson et al. divided the UVMs from TCGA

into two groups, monosomy 3 UM and disomy 3 UM, according to the gene type, and found the prognosis was different between these two groups [47]. In our study, we divided the UVMs into two groups according to the survival time and we used a LASSO Cox regression model to build a prognostic classifier and then calculated a risk score for each patient based on their own methylation levels of 13 sites in miRNAs or methylation levels of 9 sites in lncRNAs. The UVMs also were divided into high-risk and low-risk groups based on the median of the risk scores, finding that patients with a high-risk score have a greater likelihood of worse prognosis. The tdROC analysis suggested that our prognostic tools had good performance in predicting 1 year, 2 years and 3 years overall survival of UVMs.

Previous studies have identified multiple miRNAs and lncRNAs were associated with the regulation of UVMs. Aberrant DNA methylation of some genes has been

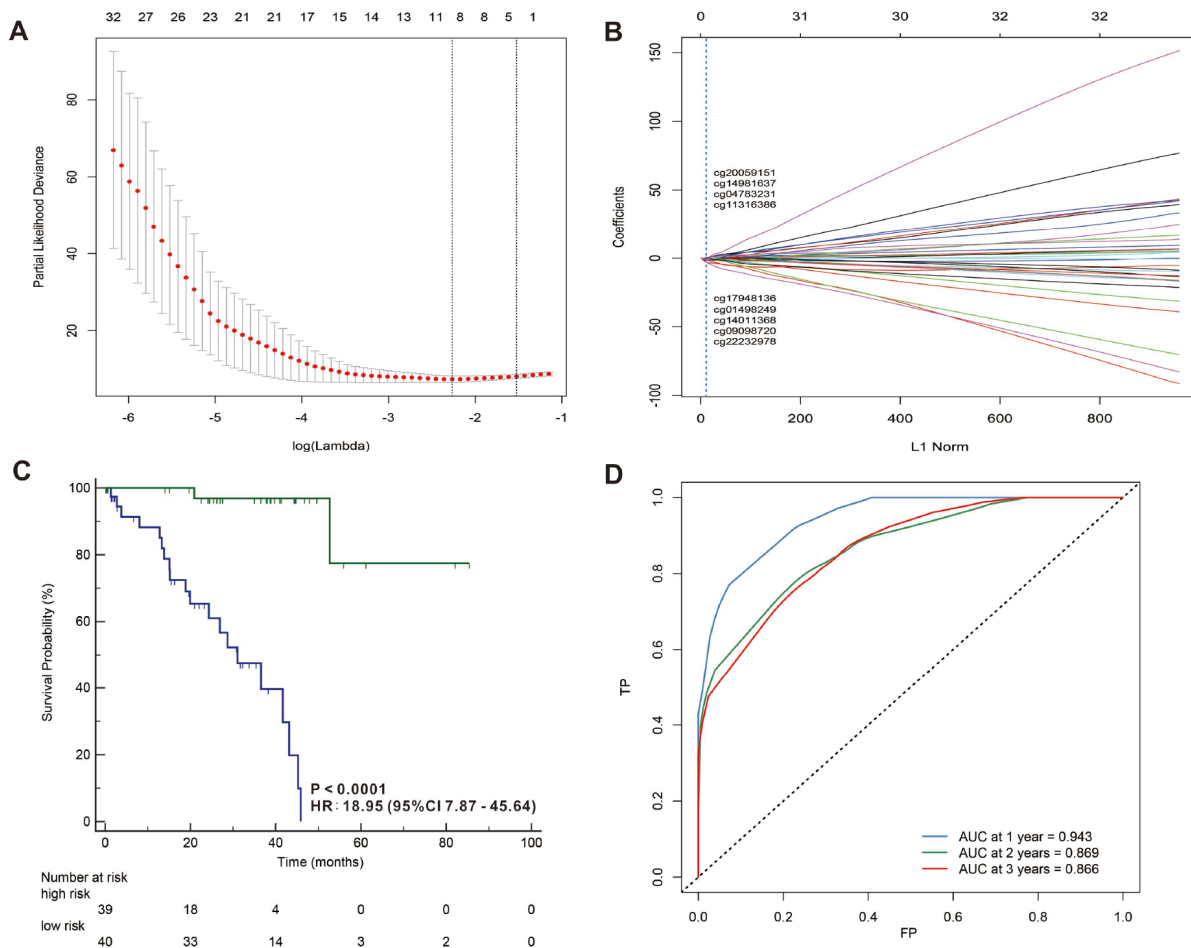


Figure 6. LASSO coefficient profiles of the 32 UVMs-associated lncRNAs (A, B). Kaplan-Meier survival analysis for all 79 patients with UVMs according to the and 9-lncRNAs-classifier stratified by clinicopathological risk factors (C). Time-dependent ROC curves by 9-lncRNAs-classifier for survival probability (D).

proved to be associated with the repression in many cancers. Therefore, based on the methylated panel analysis of miRNAs and lncRNAs, aberrantly methylated miRNAs and lncRNAs were integrated into two prognostic tools by LASSO Cox regression model with high prognostic accuracy. The biological function of the miRNAs and lncRNAs used in our classifiers have been investigated in many previous studies proved to be related to other cancers. The gene symbol of miRNA CpG sites cg07815521 is miR-641, and Tingting Y et al. found the relationship between hypermethylation of miR-641 and HPV infection in cervical cell lines [48]. Kahlert C et al. validated the liver invasion front-specific downregulation of miR-1275 (cg18007341) in colorectal liver metastases plays a pivotal role in tumor progression [49]. MiR-154 (cg21492137) proved to inhibit migration and invasion of human non-small cell lung cancer [50]. As for lncRNAs, the overexpression of TUNAR (cg14011368) significantly inhibited glioma malignancy [51]. lncRNAs can interact with miRNAs as competing for endogenous RNAs (ceRNAs) to regulate the expression of target genes in various cancers [52, 53]. Whereas miRNA can regulate lncRNA to exert biological functions by RNA-induced silencing complex (RISC). The interaction between lncRNA and miRNA participates in the occurrence of various diseases together. In this study, we found the methylated sites of miRNAs highly interacted with lncRNAs sites (Supplementary Table 1).

The current study had some limitations which can be explored in the future. First, the prognostic results based on methylation panel analysis were analyzed from UVMs data from TCGA, so the accuracy of the prediction panel should be validated using an external clinical data set. Second, the samples size of our study was somewhat small. Considering the disease occurrence of UVMs, the sample sizes in different regions need to be added. Third, in this study, we used the uveal melanoma tissues for identifying the prognostic biomarkers which have been validated the extraction of the methylated miRNA and lncRNA to ensure we can use our prognostic panel. but the blood specimen is much easier to get in the clinic and more convenient for the follow-up. If our methylated miRNAs and lncRNAs can be extracted from blood specimen, it will be a promising detection method. Thus, larger prospective trials including diverse ethnic populations with a consistent sampling protocol would be needed to confirm the validity of these biomarkers in the future.

In summary, genome-wide methylation patterns of miRNAs and lncRNAs which were related to prognosis were identified in patients with UVMs. Among these aberrantly methylated sites of miRNAs and lncRNAs, a

miRNAs-CpG-classifier and a lncRNAs-CpG-classifier for predicting the overall survival were developed, which could provide novel insights for developing biomarkers of prognosis for UVMs.

MATERIALS AND METHODS

Database of UVMs patients

DNA methylation profiles, miRNA-Seq data, RNA-seq data and clinical information of UVMs samples were extracted from the TCGA database on March 2018. The DNA methylation profiling data were performed using Infinium 450k Chip. MiRNA-Seq and RNA-seq were executed on Illumina-HiSeq miRNA-seq and RNA-seq platform. The annotation of the lncRNA file was downloaded from GENCODE (<https://www.encodegenes.org/>). We divided TCGA UVMs patients into two groups based on the survival time: Alive < 2 years group (survival time was less than 2 years after diagnose) and Alive > 2 years group (survival time was more than 2 years after diagnose).

Differentially methylated sites of miRNA and lncRNA

The DNA methylation profiles of 45 alive > 2 years and 12 alive < 2 years UVM patients were analyzed for determining methylated sites of miRNAs and lncRNAs. CpG sites in 2kb upstream of transcriptional start site (TSS) of miRNA or lncRNA were selected from 485577 sites from 450k Chip. We employed the "minfi" package to analyze methylation data by R software for differential methylated sites. Differentially methylated sites of miRNAs or lncRNAs between Alive < 2 years group and Alive > 2 years group were determined by calculating an exact beta-value. Hierarchical clustering (HC) analysis was performed with the R software with "pheatmap" package.

Bioinformatic functional analysis of differentially methylated miRNAs and lncRNAs

Target genes of miRNAs with differentially methylated sites were selected to perform prediction analysis using TargetScan (<http://www.targetscan.org/>), DIANA microT-CDS (<http://diana.imis.athena-innovation.gr/>) and miRDB (<http://mirdb.org/miRDB/>). And co-expressing genes of lncRNAs with differentially methylated sites were selected to do prediction analysis by MEM (Multi-Experiment Matrix). The function enrichment analysis of the target genes was performed through the R software with "clusterProfiler" package. LncBase (http://carolina.imis.athena-innovation.gr/diana_tools/web/index.php?r=lnccbasev2/index) was used to predict the interaction of miRNAs and lncRNAs.

Methylation patterns of miRNAs and lncRNAs associated prognosis in UVMs

We used a least absolute shrinkage and selection operator (LASSO) Cox regression model to select the most meaningful predictive CpGs and build methylation-based classifiers using the sum of methylation levels of the selected CpGs weighted by the coefficients to predict mortality. A risk score for each patient was calculated based on their individual methylated levels of the CpG sites. Using the median of the risk scores, patients were divided into high-risk and low-risk groups. Kaplan-Meier method was used to estimate the survival probability. Time-dependent receiver operating characteristic (tdROC) analysis was used for assessing the prognostic accuracy of the classifiers.

Statistical analysis

We compared two groups using the t-test (the normal distribution has been tested before) for continuous variables and χ^2 test for categorical variables. A P value less than 0.05 was considered statistically significant. Q-value less than 0.05 was considered statistically significant. Different beta-value of more than 0.1 in two groups were considered statistically significant. FDR less than 0.05 were considered significant.

Abbreviations

UVMs: Uveal melanomas; miRNAs: microRNAs; lncRNAs: long ncRNAs; TCGA: The Cancer Genome Atlas; LASSO: least absolute shrinkage and selection operator method; tdROC: Time-dependent Receiver Operating Characteristic curve; MAPK: mitogen-activated protein kinase; TSS: transcriptional start site; HC: Hierarchical clustering.

AUTHOR CONTRIBUTIONS

ZZ, DX, KS and FL conceived the study; ZZ, DX, and KS carried out the experiments; ZZ, DX, KS and MC collected and analyzed the data. ZZ, DX, MC and FL wrote the manuscript. All authors read and approved the final manuscript.

CONFLICTS OF INTEREST

All authors declare no conflicts of interest. This study has not been published previously.

FUNDING

This work was supported by grants from the National Key Research and Development Program of China

(2016YFE0107000) and the Wenzhou Science and Technology Bureau Project (Y20180171).

REFERENCES

1. Stang A, Parkin DM, Ferlay J, Jöckel KH. International uveal melanoma incidence trends in view of a decreasing proportion of morphological verification. *Int J Cancer*. 2005; 114:114–23. <https://doi.org/10.1002/ijc.20690> PMID:15523698
2. Shields CL, Shields JA, Materin M, Gershenbaum E, Singh AD, Smith A. Iris melanoma: risk factors for metastasis in 169 consecutive patients. *Ophthalmology*. 2001; 108:172–78. [https://doi.org/10.1016/S0161-6420\(00\)00449-8](https://doi.org/10.1016/S0161-6420(00)00449-8) PMID:11150284
3. Thompson JF, Scolyer RA, Kefford RF. Cutaneous melanoma. *Lancet*. 2005; 365:687–701. [https://doi.org/10.1016/S0140-6736\(05\)70937-5](https://doi.org/10.1016/S0140-6736(05)70937-5) PMID:15721476
4. Bergman L, Seregard S, Nilsson B, Lundell G, Ringborg U, Ragnarsson-Olding B. Uveal melanoma survival in Sweden from 1960 to 1998. *Invest Ophthalmol Vis Sci*. 2003; 44:3282–87. <https://doi.org/10.1167/iovs.03-0081> PMID:12882771
5. Seregard S. Long-term survival after ruthenium plaque radiotherapy for uveal melanoma. A meta-analysis of studies including 1,066 patients. *Acta Ophthalmol Scand*. 1999; 77:414–17. <https://doi.org/10.1034/j.1600-0420.1999.770411.x> PMID:10463412
6. Diener-West M, Hawkins BS, Markowitz JA, Schachat AP. A review of mortality from choroidal melanoma. II. A meta-analysis of 5-year mortality rates following enucleation, 1966 through 1988. *Arch Ophthalmol*. 1992; 110:245–50. <https://doi.org/10.1001/archophth.1992.01080140101036> PMID:1531290
7. Singh AD, Turell ME, Topham AK. Uveal melanoma: trends in incidence, treatment, and survival. *Ophthalmology*. 2011; 118:1881–85. <https://doi.org/10.1016/j.ophtha.2011.01.040> PMID:21704381
8. Ambros V. The functions of animal microRNAs. *Nature*. 2004; 431:350–55. <https://doi.org/10.1038/nature02871> PMID:15372042
9. Bartel DP. MicroRNAs: genomics, biogenesis, mechanism, and function. *Cell*. 2004; 116:281–97. [https://doi.org/10.1016/S0092-8674\(04\)00045-5](https://doi.org/10.1016/S0092-8674(04)00045-5) PMID:14744438

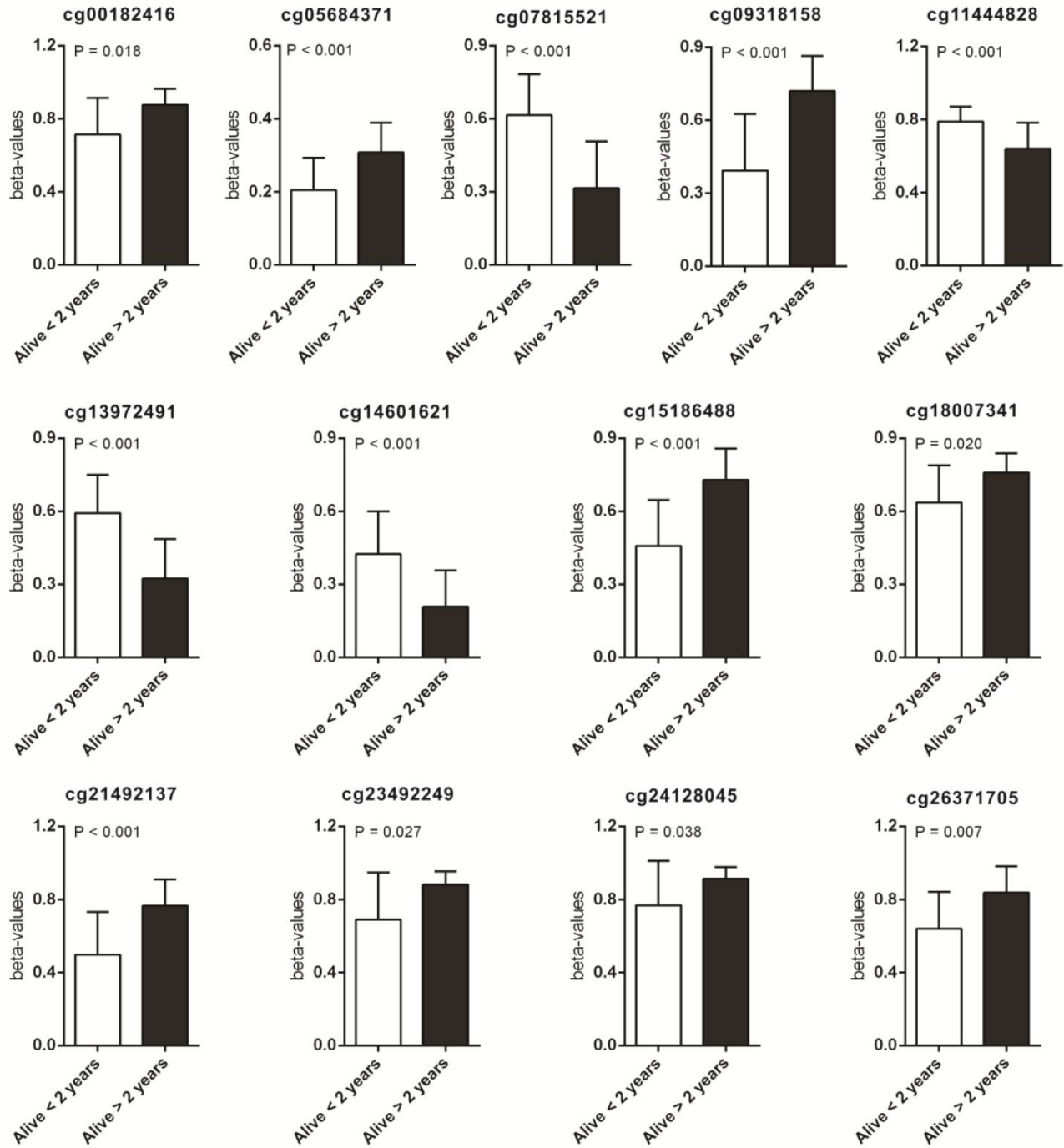
10. Perkel JM. Visiting “noncodarnia”. *Biotechniques*. 2013; 54:301, 303–04.
<https://doi.org/10.2144/000114037> PMID:[23750541](https://pubmed.ncbi.nlm.nih.gov/23750541/)
11. Iorio MV, Croce CM. MicroRNA dysregulation in cancer: diagnostics, monitoring and therapeutics. A comprehensive review. *EMBO Mol Med*. 2012; 4:143–59.
<https://doi.org/10.1002/emmm.201100209> PMID:[22351564](https://pubmed.ncbi.nlm.nih.gov/22351564/)
12. Liu Y, Zhao M. InCaNet: pan-cancer co-expression network for human lncRNA and cancer genes. *Bioinformatics*. 2016; 32:1595–97.
<https://doi.org/10.1093/bioinformatics/btw017> PMID:[26787663](https://pubmed.ncbi.nlm.nih.gov/26787663/)
13. Zhuo ZJ, Zhang R, Zhang J, Zhu J, Yang T, Zou Y, He J, Xia H. Associations between lncRNA *MEG3* polymorphisms and neuroblastoma risk in Chinese children. *Aging (Albany NY)*. 2018; 10:481–91.
<https://doi.org/10.18632/aging.101406> PMID:[29615542](https://pubmed.ncbi.nlm.nih.gov/29615542/)
14. Sun KY, Peng T, Chen Z, Song P, Zhou XH. Long non-coding RNA LOC100129148 functions as an oncogene in human nasopharyngeal carcinoma by targeting miR-539-5p. *Aging (Albany NY)*. 2017; 9:999–1011.
<https://doi.org/10.18632/aging.101205> PMID:[28328537](https://pubmed.ncbi.nlm.nih.gov/28328537/)
15. Zhou H, Wang F, Chen H, Tan Q, Qiu S, Chen S, Jing W, Yu M, Liang C, Ye S, Tu J. Increased expression of long-noncoding RNA ZFAS1 is associated with epithelial-mesenchymal transition of gastric cancer. *Aging (Albany NY)*. 2016; 8:2023–38.
<https://doi.org/10.18632/aging.101048> PMID:[27654478](https://pubmed.ncbi.nlm.nih.gov/27654478/)
16. Yan D, Dong XD, Chen X, Yao S, Wang L, Wang J, Wang C, Hu DN, Qu J, Tu L. Role of microRNA-182 in posterior uveal melanoma: regulation of tumor development through MITF, BCL2 and cyclin D2. *PLoS One*. 2012; 7:e40967.
<https://doi.org/10.1371/journal.pone.0040967> PMID:[22848417](https://pubmed.ncbi.nlm.nih.gov/22848417/)
17. Liu N, Sun Q, Chen J, Li J, Zeng Y, Zhai S, Li P, Wang B, Wang X. MicroRNA-9 suppresses uveal melanoma cell migration and invasion through the NF- κ B1 pathway. *Oncol Rep*. 2012; 28:961–68.
<https://doi.org/10.3892/or.2012.1905> PMID:[22825752](https://pubmed.ncbi.nlm.nih.gov/22825752/)
18. Yan D, Zhou X, Chen X, Hu DN, Dong XD, Wang J, Lu F, Tu L, Qu J. MicroRNA-34a inhibits uveal melanoma cell proliferation and migration through downregulation of c-Met. *Invest Ophthalmol Vis Sci*. 2009; 50:1559–65.
<https://doi.org/10.1167/iovs.08-2681> PMID:[19029026](https://pubmed.ncbi.nlm.nih.gov/19029026/)
19. Chen X, Wang J, Shen H, Lu J, Li C, Hu DN, Dong XD, Yan D, Tu L. Epigenetics, microRNAs, and carcinogenesis: functional role of microRNA-137 in uveal melanoma. *Invest Ophthalmol Vis Sci*. 2011; 52:1193–99.
<https://doi.org/10.1167/iovs.10-5272> PMID:[21051724](https://pubmed.ncbi.nlm.nih.gov/21051724/)
20. Sun L, Sun P, Zhou QY, Gao X, Han Q. Long noncoding RNA MALAT1 promotes uveal melanoma cell growth and invasion by silencing of miR-140. *Am J Transl Res*. 2016; 8:3939–46. PMID:[27725873](https://pubmed.ncbi.nlm.nih.gov/27725873/)
21. Ding X, Wang X, Lin M, Xing Y, Ge S, Jia R, Zhang H, Fan X, Li J. PAUPAR lncRNA suppresses tumorigenesis by H3K4 demethylation in uveal melanoma. *FEBS Lett*. 2016; 590:1729–38.
<https://doi.org/10.1002/1873-3468.12220> PMID:[27214741](https://pubmed.ncbi.nlm.nih.gov/27214741/)
22. Esteller M. Dormant hypermethylated tumour suppressor genes: questions and answers. *J Pathol*. 2005; 205:172–80.
<https://doi.org/10.1002/path.1707> PMID:[15643671](https://pubmed.ncbi.nlm.nih.gov/15643671/)
23. Yu L. [DNA methylation and cancer]. *Zhonghua Nei Ke Za Zhi*. 2005; 44:403–04. DNA methylation and cancer PMID:[16008842](https://pubmed.ncbi.nlm.nih.gov/16008842/)
24. Laird PW. The power and the promise of DNA methylation markers. *Nat Rev Cancer*. 2003; 3:253–66.
<https://doi.org/10.1038/nrc1045> PMID:[12671664](https://pubmed.ncbi.nlm.nih.gov/12671664/)
25. Sato F, Tsuchiya S, Meltzer SJ, Shimizu K. MicroRNAs and epigenetics. *FEBS J*. 2011; 278:1598–609.
<https://doi.org/10.1111/j.1742-4658.2011.08089.x> PMID:[21395977](https://pubmed.ncbi.nlm.nih.gov/21395977/)
26. Yim RL, Kwong YL, Wong KY, Chim CS. DNA Methylation of Tumor Suppressive miRNAs in Non-Hodgkin’s Lymphomas. *Front Genet*. 2012; 3:233.
<https://doi.org/10.3389/fgene.2012.00233> PMID:[23162567](https://pubmed.ncbi.nlm.nih.gov/23162567/)
27. Pinto R, De Summa S, Pilato B, Tommasi S. DNA methylation and miRNAs regulation in hereditary breast cancer: epigenetic changes, players in transcriptional and post-transcriptional regulation in hereditary breast cancer. *Curr Mol Med*. 2014; 14:45–57.
<https://doi.org/10.2174/1566524013666131203101405> PMID:[24295492](https://pubmed.ncbi.nlm.nih.gov/24295492/)
28. Ma X, Yu L, Wang P, Yang X. Discovering DNA methylation patterns for long non-coding RNAs associated with cancer subtypes. *Comput Biol Chem*. 2017; 69:164–70.
<https://doi.org/10.1016/j.compbiolchem.2017.03.014> PMID:[28501295](https://pubmed.ncbi.nlm.nih.gov/28501295/)

29. Yang ZK, Yang JY, Xu ZZ, Yu WH. DNA Methylation and Uveal Melanoma. *Chin Med J (Engl)*. 2018; 131:845–51.
<https://doi.org/10.4103/0366-6999.228229>
PMID:[29578129](https://pubmed.ncbi.nlm.nih.gov/29578129/)
30. Fromm B, Billipp T, Peck LE, Johansen M, Tarver JE, King BL, Newcomb JM, Sempere LF, Flatmark K, Hovig E, Peterson KJ. A Uniform System for the Annotation of Vertebrate microRNA Genes and the Evolution of the Human microRNAome. *Annu Rev Genet*. 2015; 49:213–42.
<https://doi.org/10.1146/annurev-genet-120213-092023> PMID:[26473382](https://pubmed.ncbi.nlm.nih.gov/26473382/)
31. Bartel DP. MicroRNAs: target recognition and regulatory functions. *Cell*. 2009; 136:215–33.
<https://doi.org/10.1016/j.cell.2009.01.002>
PMID:[19167326](https://pubmed.ncbi.nlm.nih.gov/19167326/)
32. Fabian MR, Sonenberg N, Filipowicz W. Regulation of mRNA translation and stability by microRNAs. *Annu Rev Biochem*. 2010; 79:351–79.
<https://doi.org/10.1146/annurev-biochem-060308-103103> PMID:[20533884](https://pubmed.ncbi.nlm.nih.gov/20533884/)
33. Dinger ME, Amaral PP, Mercer TR, Pang KC, Bruce SJ, Gardiner BB, Askarian-Amiri ME, Ru K, Soldà G, Simons C, Sunkin SM, Crowe ML, Grimmond SM, et al. Long noncoding RNAs in mouse embryonic stem cell pluripotency and differentiation. *Genome Res*. 2008; 18:1433–45.
<https://doi.org/10.1101/gr.078378.108>
PMID:[18562676](https://pubmed.ncbi.nlm.nih.gov/18562676/)
34. Nagano T, Fraser P. No-nonsense functions for long noncoding RNAs. *Cell*. 2011; 145:178–81.
<https://doi.org/10.1016/j.cell.2011.03.014>
PMID:[21496640](https://pubmed.ncbi.nlm.nih.gov/21496640/)
35. Jaenisch R, Bird A. Epigenetic regulation of gene expression: how the genome integrates intrinsic and environmental signals. *Nat Genet*. 2003 (Suppl); 33:245–54.
<https://doi.org/10.1038/ng1089>
PMID:[12610534](https://pubmed.ncbi.nlm.nih.gov/12610534/)
36. Fresno Vara JA, Casado E, de Castro J, Cejas P, Beldarrain C, González-Barón M. PI3K/Akt signalling pathway and cancer. *Cancer Treat Rev*. 2004; 30:193–204.
<https://doi.org/10.1016/j.ctrv.2003.07.007>
PMID:[15023437](https://pubmed.ncbi.nlm.nih.gov/15023437/)
37. Hennessey BT, Smith DL, Ram PT, Lu Y, Mills GB. Exploiting the PI3K/AKT pathway for cancer drug discovery. *Nat Rev Drug Discov*. 2005; 4:988–1004.
<https://doi.org/10.1038/nrd1902> PMID:[16341064](https://pubmed.ncbi.nlm.nih.gov/16341064/)
38. Fecher LA, Amaravadi RK, Flaherty KT. The MAPK pathway in melanoma. *Curr Opin Oncol*. 2008; 20:183–89.
<https://doi.org/10.1097/CCO.0b013e3282f5271c>
PMID:[18300768](https://pubmed.ncbi.nlm.nih.gov/18300768/)
39. Giehl K. Oncogenic Ras in tumour progression and metastasis. *Biol Chem*. 2005; 386:193–205.
<https://doi.org/10.1515/BC.2005.025>
PMID:[15843165](https://pubmed.ncbi.nlm.nih.gov/15843165/)
40. Gold MG, Gonen T, Scott JD. Local cAMP signaling in disease at a glance. *J Cell Sci*. 2013; 126:4537–43.
<https://doi.org/10.1242/jcs.133751>
PMID:[24124191](https://pubmed.ncbi.nlm.nih.gov/24124191/)
41. Murray F, Insel PA. Targeting cAMP in chronic lymphocytic leukemia: a pathway-dependent approach for the treatment of leukemia and lymphoma. *Expert Opin Ther Targets*. 2013; 17:937–49.
<https://doi.org/10.1517/14728222.2013.798304>
PMID:[23647244](https://pubmed.ncbi.nlm.nih.gov/23647244/)
42. Park JY, Juhn YS. cAMP signaling increases histone deacetylase 8 expression via the Epac2-Rap1A-Akt pathway in H1299 lung cancer cells. *Exp Mol Med*. 2017; 49:e297.
<https://doi.org/10.1038/emm.2016.152>
PMID:[28232663](https://pubmed.ncbi.nlm.nih.gov/28232663/)
43. Prevarskaya N, Skryma R, Shuba Y. Calcium in tumour metastasis: new roles for known actors. *Nat Rev Cancer*. 2011; 11:609–18.
<https://doi.org/10.1038/nrc3105> PMID:[21779011](https://pubmed.ncbi.nlm.nih.gov/21779011/)
44. Monteith GR, McAndrew D, Faddy HM, Roberts-Thomson SJ. Calcium and cancer: targeting Ca²⁺ transport. *Nat Rev Cancer*. 2007; 7:519–30.
<https://doi.org/10.1038/nrc2171> PMID:[17585332](https://pubmed.ncbi.nlm.nih.gov/17585332/)
45. Kath R, Hayungs J, Bornfeld N, Sauerwein W, Höffken K, Seeber S. Prognosis and treatment of disseminated uveal melanoma. *Cancer*. 1993; 72:2219–23.
[https://doi.org/10.1002/1097-0142\(19931001\)72:7<2219::AID-CNCR2820720725>3.0.CO;2-J](https://doi.org/10.1002/1097-0142(19931001)72:7<2219::AID-CNCR2820720725>3.0.CO;2-J) PMID:[7848381](https://pubmed.ncbi.nlm.nih.gov/7848381/)
46. Kujala E, Mäkitie T, Kivelä T. Very long-term prognosis of patients with malignant uveal melanoma. *Invest Ophthalmol Vis Sci*. 2003; 44:4651–59.
<https://doi.org/10.1167/iovs.03-0538>
PMID:[14578381](https://pubmed.ncbi.nlm.nih.gov/14578381/)
47. Robertson AG, Shih J, Yau C, Gibb EA, Oba J, Mungall KL, Hess JM, Uzunangelov V, Walter V, Danilova L, Lichtenberg TM, Kucherlapati M, Kimes PK, et al. Integrative Analysis Identifies Four Molecular and Clinical Subsets in Uveal Melanoma. *Cancer Cell*. 2017; 32:204–20.e15.
<https://doi.org/10.1016/j.ccell.2017.07.003>
PMID:[28810145](https://pubmed.ncbi.nlm.nih.gov/28810145/)
48. Yao T, Rao Q, Liu L, Zheng C, Xie Q, Liang J, Lin Z.

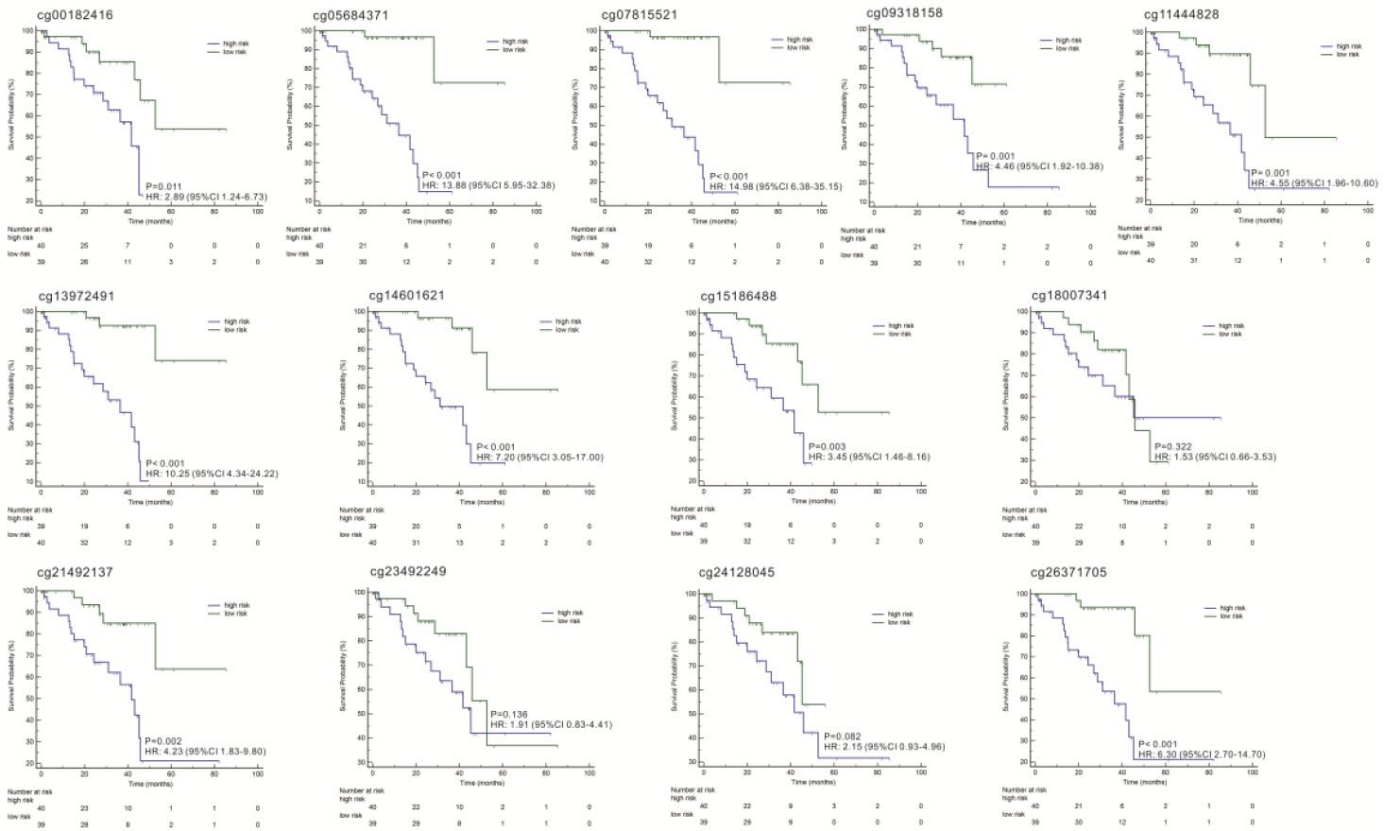
- Exploration of tumor-suppressive microRNAs silenced by DNA hypermethylation in cervical cancer. *Virology*. 2013; 10:175.
<https://doi.org/10.1186/1743-422X-10-175>
PMID:[23732000](https://pubmed.ncbi.nlm.nih.gov/23732000/)
49. Kahlert C, Klupp F, Brand K, Lasitschka F, Diederichs S, Kirchberg J, Rahbari N, Dutta S, Bork U, Fritzmann J, Reissfelder C, Koch M, Weitz J. Invasion front-specific expression and prognostic significance of microRNA in colorectal liver metastases. *Cancer Sci*. 2011; 102:1799–807.
<https://doi.org/10.1111/j.1349-7006.2011.02023.x>
PMID:[21722265](https://pubmed.ncbi.nlm.nih.gov/21722265/)
50. Lin X, Yang Z, Zhang P, Liu Y, Shao G. miR-154 inhibits migration and invasion of human non-small cell lung cancer by targeting ZEB2. *Oncol Lett*. 2016; 12:301–06.
<https://doi.org/10.3892/ol.2016.4577>
PMID:[27347142](https://pubmed.ncbi.nlm.nih.gov/27347142/)
51. Dai J, Ma J, Yu B, Zhu Z, Hu Y. Long non-coding RNA TUNAR represses growth, migration and invasion of human glioma cells through regulating miR-200a and Rac1. *Oncol Res*. 2018; 27:107–15.
<https://doi.org/10.3727/096504018X15205622257163> PMID:[29540255](https://pubmed.ncbi.nlm.nih.gov/29540255/)
52. Tay Y, Rinn J, Pandolfi PP. The multilayered complexity of ceRNA crosstalk and competition. *Nature*. 2014; 505:344–52.
<https://doi.org/10.1038/nature12986>
PMID:[24429633](https://pubmed.ncbi.nlm.nih.gov/24429633/)
53. Guo G, Kang Q, Zhu X, Chen Q, Wang X, Chen Y, Ouyang J, Zhang L, Tan H, Chen R, Huang S, Chen JL. A long noncoding RNA critically regulates Bcr-Abl-mediated cellular transformation by acting as a competitive endogenous RNA. *Oncogene*. 2015; 34:1768–79. <https://doi.org/10.1038/onc.2014.131>
PMID:[24837367](https://pubmed.ncbi.nlm.nih.gov/24837367/)

SUPPLEMENTARY MATERIALS

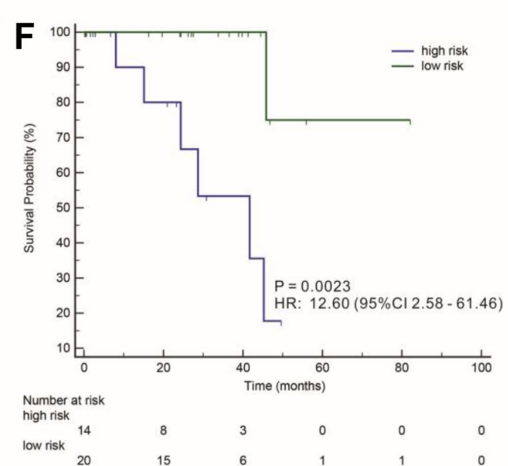
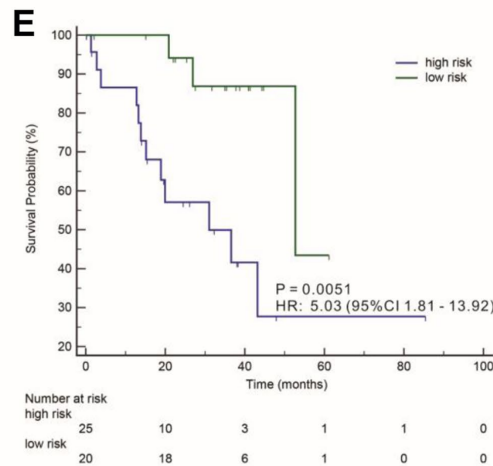
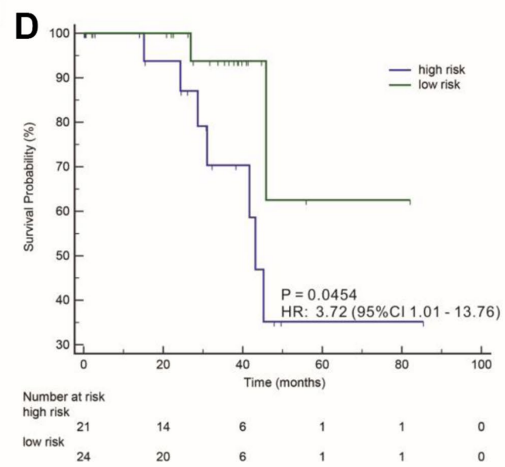
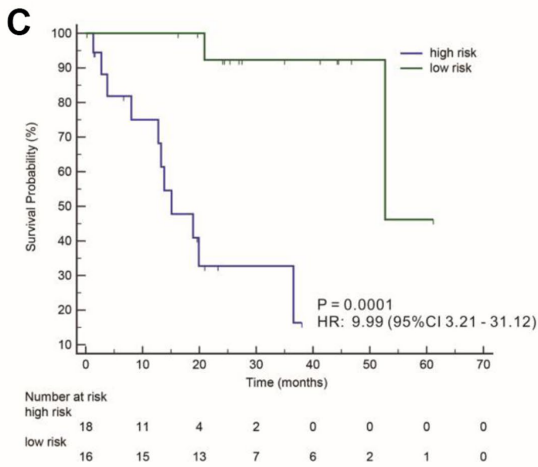
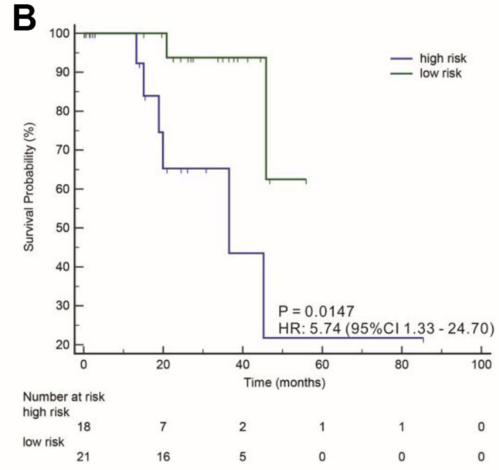
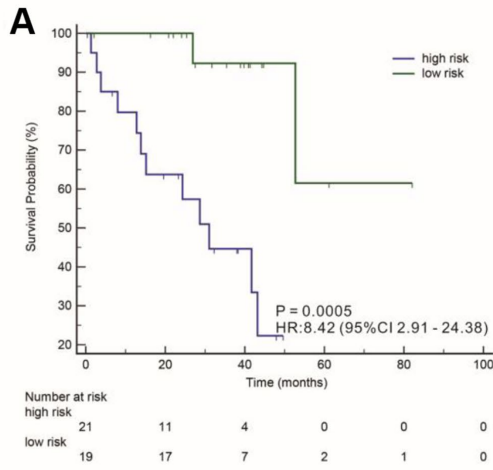
Supplementary Figures



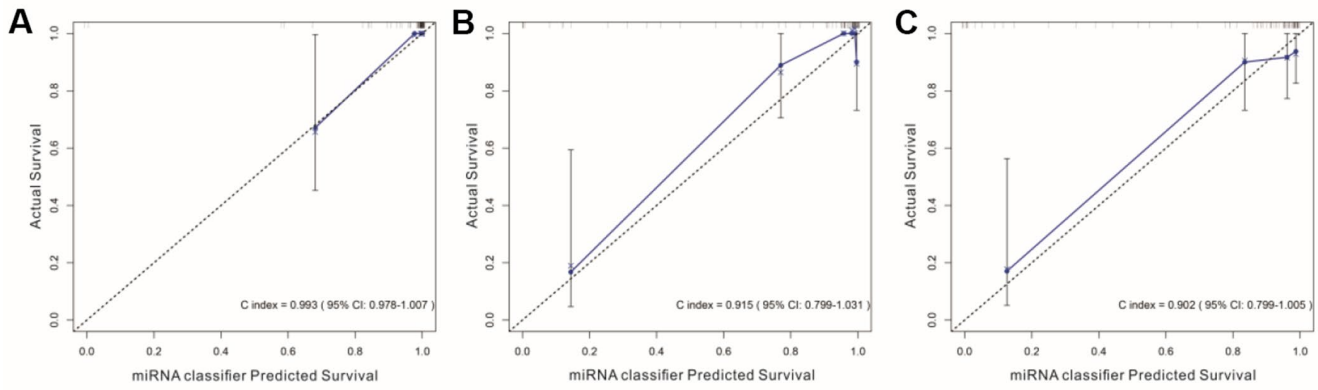
Supplementary Figure 1. Aberrantly methylated miRNAs target genes of different prognosis group of UVMs. The screened out 13 miRNA CpG sites from the 45 miRNA CpG sites of alive > 2 years and alive < 2 years UVM patients.



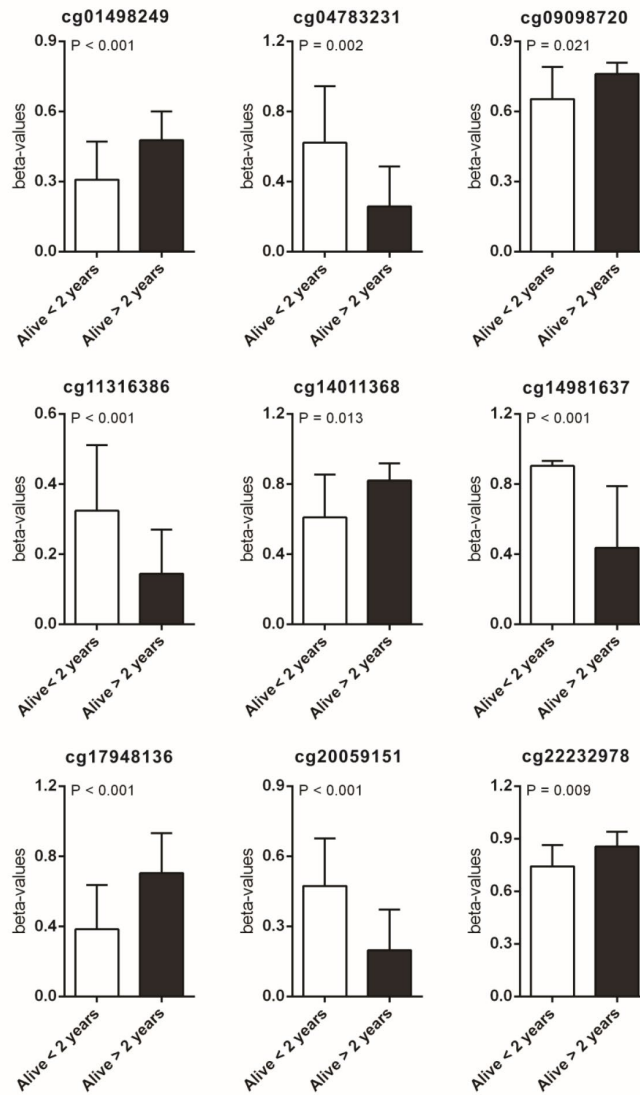
Supplementary Figure 2. Kaplan-Meier survival analysis for UVMs according to the screened out 13 miRNA CpG sites.



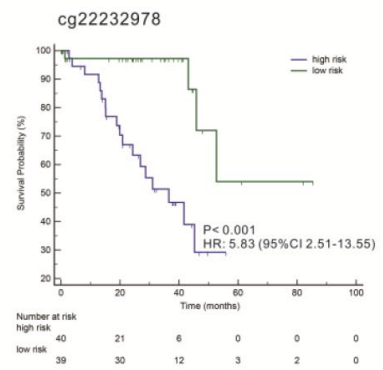
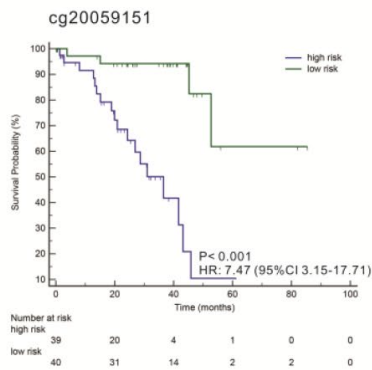
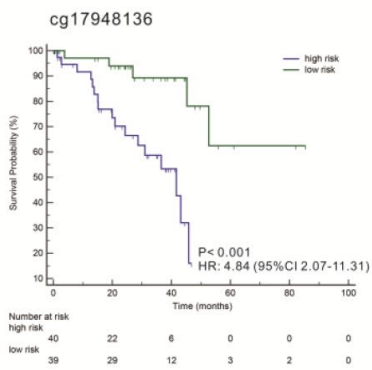
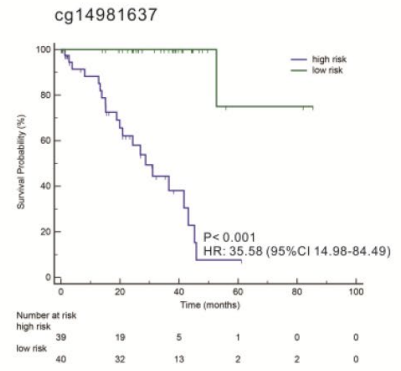
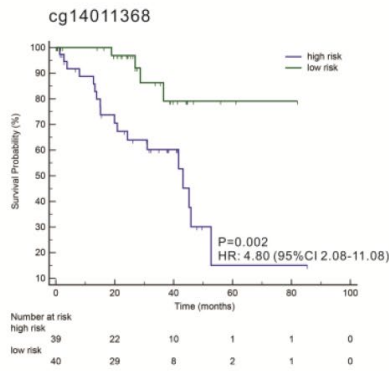
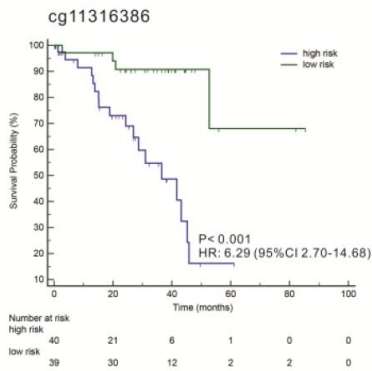
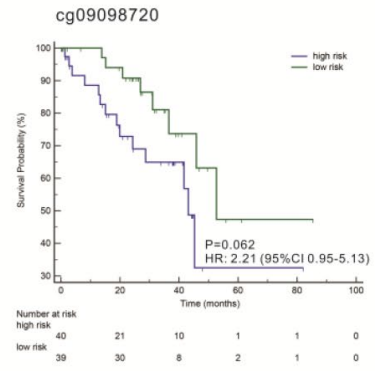
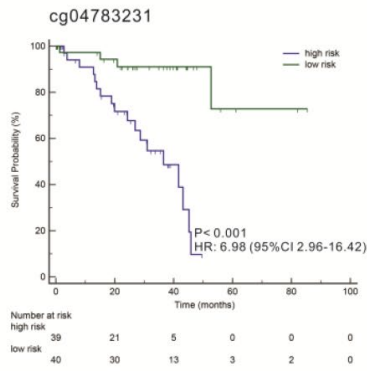
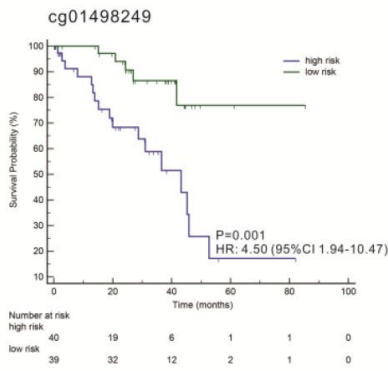
Supplementary Figure 3. Kaplan-Meier survival analysis for UVMs according to the different miRNAs-classifiers.



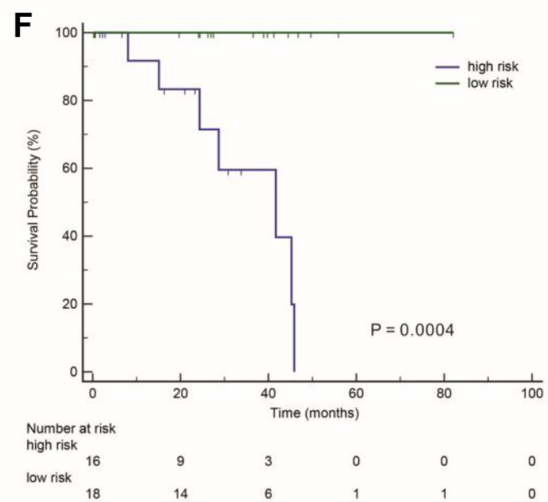
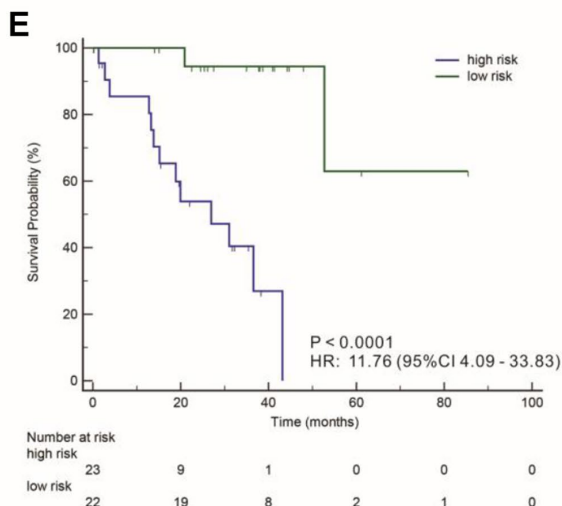
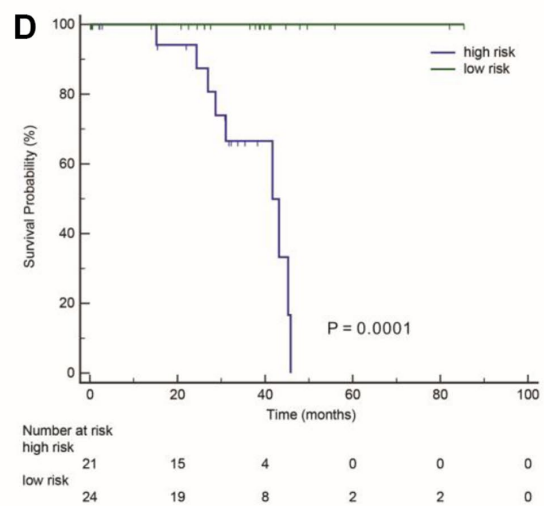
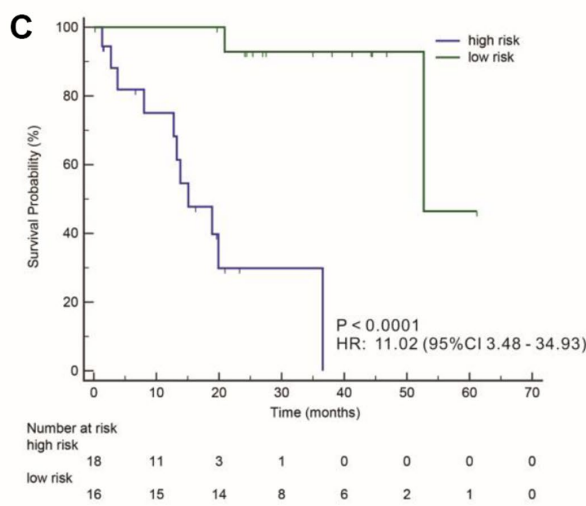
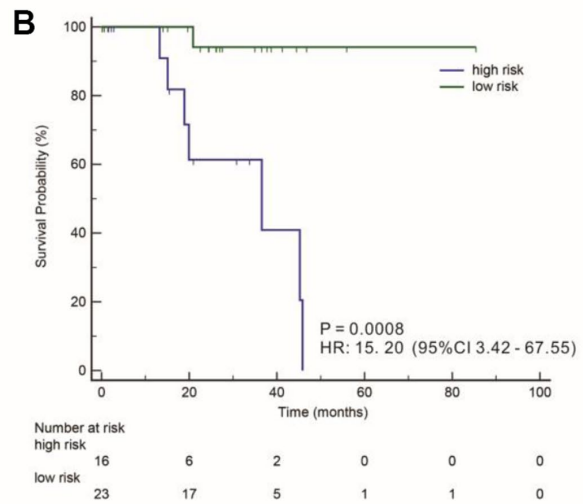
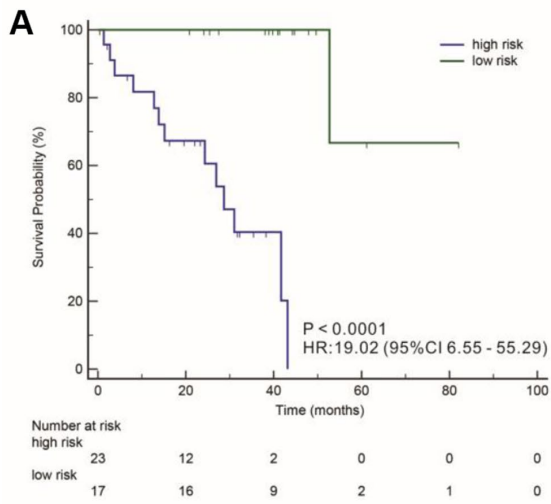
Supplementary Figure 4. Calibration of miRNAs-CpG-classifier.



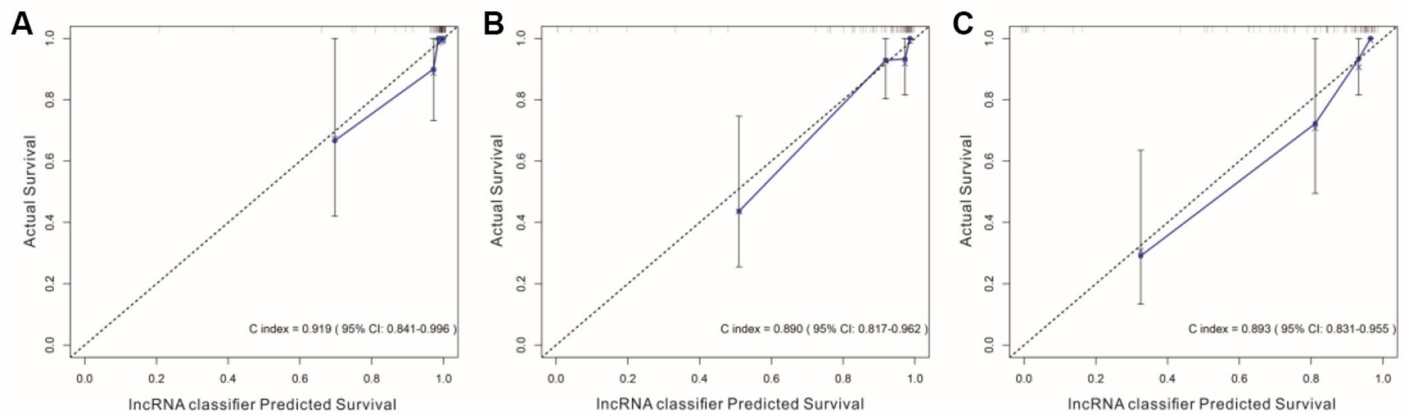
Supplementary Figure 5. Aberrantly methylated genes co-expressing with lncRNAs of different prognosis group of UVMs. The screened out 9 lncRNA CpG sites from the 33 lncRNA CpG sites of alive > 2 years and alive < 2 years UVM patients.



Supplementary Figure 6. Kaplan-Meier survival analysis for UVMs according to the screened out 9 miRNA CpG sites.



Supplementary Figure 7. Kaplan-Meier survival analysis for UVMs according to the different lncRNAs-classifiers.



Supplementary Figure 8. Calibration of lncRNAs-CpG-classifier.

Supplementary Tables

Supplementary Table 1. Interaction of lncRNA signature with miRNA signature by prediction.

Gene symbols of lncRNA	Gene symbols of miRNA
AC007228.5	miR-516a
AC011516.2	miR-515, miR-519e
AC079586.1	miR-299, miR-3074, miR-372, miR-6721
CTB-61M7.2	let-7a, miR-1323, miR-541
CTC-321K16.4	miR-299, miR-515, miR-516a, miR-519e
CTC-33909.1	miR-372, miR-373, miR-376b, miR-518a, miR-519b, miR-519c, miR-520c, miR-520d, miR-526a, miR-6754
CTD-2291D10.4	miR-512, miR-654
CTD-3022G6.1	miR-1275, miR-373, miR-519b, miR-519c, miR-520c, miR-520d, miR-526b
LINC01057	miR-3074
MEG3	let-7a, miR-495, miR-541, miR-654
MEG8	miR-379
MIR99AHG	miR-516a, miR-526b
RP11-1018N14.2	miR-1283, miR-1324, miR-3074, miR-520d
RP11-273G15.2	miR-526b
RP11-76E12.1	miR-299, miR-379, miR-515, miR-5193, miR-519e
TUNAR	miR-5193, miR-6754

Supplementary Table 2. Characteristics of miRNA CG locus filtered by LASSO.

CG_ID	Gene_symbol	CG_Chromosome_location	Position_to_TSS	CGI_coordinate	Feature_type
cg00182416	MIR516A2	chr19:53760663-53760664	TSS1500	chr19:53768486-53768705	
cg05684371	MIR1324	chr3:75629873- 75629874	TSS1500	chr3:75618626-75619916	
cg07815521	MIR641	chr19: 40283950- 40283951	TSS1500	chr19:40284830-40285700	N_Shore
cg09318158	MIR1283-1	chr19: 53688356-53688357	TSS200	chr19:53647822-53648987	
cg11444828	MIR6721	chr6: 32170196- 32170197	TSS200	chr6:32166683-32167419	S_Shelf
cg13972491	MIR3074	chr9: 95086454- 95086455	TSS1500	chr9:95085858-95086243	S_Shore
cg14601621	MIR3074	chr9: 95086175- 95086176	TSS200	chr9:95085858-95086243	Island
cg15186488	MIR518A2	chr19: 53739274- 53739275	TSS200	chr19:53768486-53768705	
cg18007341	MIR1275	chr6: 34000147- 34000148	TSS200	chr6:34028161-34028387	
cg21492137	MIR154	chr14: 101059602-	TSS200	chr14:101065306-	
	MIR496	101059603	TSS1500	101066047	
cg23492249	MIR299	chr14: 101023683-	TSS200	chr14:101065306-	
		101023684		101066047	
cg24128045	MIR1323	chr19: 53671352- 53671353	TSS1500	chr19:53647822-53648987	
cg26371705	MIRLET7A3	chr22: 46111361- 46111362	TSS1500	chr22:46122574-46122849	

CGI, CpG island.

Supplementary Table 3. Characteristics of lncRNA CG locus filtered by LASSO.

CG_ID	Gene_symbol	CG_chromosome_location	Position_to_TSS	CGI_coordinate	Feature_type
cg01498249	AC079779.5	chr2: 312940- 312941	TSS1500	chr2:314828-315170	N_Shore
cg04783231	AC005498.3	chr19: 56539465-	TSS1500	chr19:56538306-	S_Shore
		56539466		56539277	
cg09098720	RP11-1018N14.1	chr17: 51335481-	TSS1500	chr17:51259741-	
	RP11-1018N14.2	51335482	TSS1500	51261222	
cg11316386	C1orf229	chr1: 247112506-	TSS200	chr1:247111283-	S_Shore
		247112507		247112455	
cg14011368	TUNAR	chr14: 95875201-	TSS1500	chr14:95875872-	N_Shore
		95875202		95877233	
cg14981637	LINC01057	chr1: 94821571- 94821572	TSS1500	chr1:94820046-94820763	S_Shore
cg17948136	CTD-2291D10.4	chr19: 23074517-	TSS1500	chr19:23075155-	N_Shore
		23074518		23075716	
cg20059151	LINC01057	chr1: 94820755- 94820756	TSS1500	chr1:94820046-94820763	Island
cg22232978	AC096579.13	chr2: 88861913- 88861914	TSS1500	chr2:88764976-88765996	

CGI, CpG island.

Supplementary Table 4. KM analyses of miRNA CpG methylation for overall survival.

CG_ID (high vs. low risk)	HR	95% CI	P value
cg00182416	2.89	1.24-6.73	0.011
cg05684371	13.88	5.95-32.38	< 0.001
cg07815521	14.98	6.38-35.15	< 0.001
cg09318158	4.46	1.92-10.38	0.001
cg11444828	4.55	1.96-10.60	0.001
cg13972491	10.25	4.34-24.22	< 0.001
cg14601621	7.20	3.05-17.00	< 0.001
cg15186488	3.45	1.46-8.16	0.003
cg18007341	1.53	0.66-3.53	0.322
cg21492137	4.23	1.83-9.80	0.002
cg23492249	1.91	0.83-4.41	0.136
cg24128045	2.15	0.93-4.96	0.082
cg26371705	6.30	2.70-14.70	< 0.001

KM, Kaplan-Meier; HR, Hazard ratio; CI, confidence interval.

Supplementary Table 5. KM analyses of lncRNA CpG methylation for overall survival.

CG_ID (high vs. low risk)	HR	95% CI	P value
cg01498249	4.50	1.94-10.47	0.001
cg04783231	6.98	2.96-16.42	< 0.001
cg09098720	2.21	0.95-5.13	0.062
cg11316386	6.29	2.70-14.68	< 0.001
cg14011368	4.80	2.08-11.08	0.002
cg14981637	35.58	14.98-84.49	< 0.001
cg17948136	4.84	2.07-11.31	< 0.001
cg20059151	7.47	3.15-17.71	< 0.001
cg22232978	5.83	2.51-13.55	< 0.001

HR, Hazard ratio; CI, confidence interval.